Nuclear Physics A477 (1988) 523–540
North-Holland, Amsterdam

HEAVY-ION REACTION STUDIES OF ^{35,36}P

N.A. ORR, W.N. CATFORD, L.K. FIFIELD, T.R. OPHEL,
D.C. WEISSER and C.L. WOODS

Department of Nuclear Physics, Research School of Physical Sciences,
Australian National University, GPO Box 4, Canberra A.C.T. 2601, Australia

Received 21 April 1987
(Revised 7 September 1987)

Abstract: The spectroscopy of the $T_z \geq \frac{5}{2}$ nuclei ^{35}P and ^{36}P has been studied using a variety of multi-nucleon heavy-ion transfer reactions. This has led to the observation of a number of new levels in both nuclei. The probable structure of these and previously reported levels are deduced through comparison with DWBA and shell-model calculations.

E | NUCLEAR REACTIONS ^{37}Cl(^{11}B, ^{13}N), ^{37}Cl(^{13}C, ^{14}O), ^{34}S(^{18}O, ^{17}F), $E = 81$–108 MeV; measured $\sigma(E(^{13}\text{N}))$, $\sigma(E(^{14}\text{O}))$, $\sigma(E(^{17}\text{F}))$. ^{35,36}P deduced ground-state mass excess, levels. Enriched targets.

1. Introduction

As part of a program [1–3]) to investigate the properties of the neutron-rich nuclei near the $N = 20$ shell closure, new information on the level schemes of two $T_z \geq \frac{5}{2}$ phosphorus isotopes, ^{35}P and ^{36}P, has been obtained. The nuclei were populated by multi-nucleon transfer reactions, providing results that are complementary to previous studies [2,4–7]) of both nuclei via either simpler reactions or β-decay.

Previous reaction studies [2,5–7]) of ^{35}P have been confined to single-proton pick-up reactions from ^{36}S targets. The states populated by these reactions are limited to those involving the $N = 20$ closed-shell neutron configuration. In the present work, we have used the ^{34}S(^{18}O, ^{17}F)^{35}P reaction to investigate excited states in which one or more neutrons are promoted into the 1f–2p shell. In addition, the 2-proton pick-up reaction ^{37}Cl(^{11}B, ^{13}N)^{35}P has been employed in order to probe states involving proton occupancy of the $1d_{3/2}$ orbital. Recently, information on the level scheme of ^{35}P has also been forthcoming from a study [8]) of the γ-rays emitted following the β-decay of ^{35}Si and the present work may aid the derivation of a level scheme from the γ-ray data.

The only previous studies [2,5]) of the nucleus ^{36}P have been limited to charge-exchange reactions on ^{36}S targets. Although both studies provide consistent mass determinations and populate a single excited state, the excitation energies of the states, 252 and 450 keV respectively, are different. Here we report a study of the

^{37}Cl(^{13}C, ^{14}O)^{36}P reaction, which in contrast to the charge exchange reactions, should populate states with configurations containing a $1d_{3/2}$ proton. Again, the information obtained in the present work may assist in the interpretation of the γ-ray data of Dufour *et al.* [8]) arising from the β-decay of ^{36}Si.

2. Experimental techniques

Beams of 108 MeV $^{18}O^{7+}$, 94.5 MeV $^{13}C^{6+}$ and 81 MeV $^{11}B^{5+}$ ions from the ANU 14UD Pelletron accelerator were used to bombard various thin isotopically enriched targets (table 1). The beam current on target was typically 200 nA. Reaction products were momentum analysed by an Enge split-pole spectrometer positioned at a mean reaction angle of 8.0°, subtending a solid angle of 3.4 msr at the target with a 4.5° acceptance in the reaction plane. The total energy, rate of energy loss, position and angle of incidence of each ion arriving at the focal plane were determined using a multi-element gas-filled detector [9]). These quantities allowed the clean separation of the various ion species. Since the entrance aperture of the spectrometer spans a range of reaction angles (5.75°–10.25°), the angle-of-entry information is required to verify the correct kinematic dependence on angle for peaks assigned to levels in the nucleus under study. This is demonstrated in fig. 1d where reaction products with the correct kinematic dependence on angle are focused at the position sensing wire and form vertical lines. In order to reduce the counting rate in the 60-cm long detector to less than 1000 s^{-1}, thick absorbers were used to mask off all but the regions of interest on the focal plane.

Some difficulty was experienced in producing chloride targets which were stable under beam bombardment. Targets of barium chloride on carbon backings were

TABLE 1

Targets

Reaction	Target	Composition (μgms/cm^2) [a])				Isotopic enrichment
		C	S	Cl	Ag	
^{34}S(^{18}O^{17}F)^{35}P	$Ag_2^{34}S$	20	22		111	95%
	$Ag_2^{32}S$	20	18		108	>99.8%
^{37}Cl(^{11}B, ^{13}N)^{35}P	$Ba^{37}Cl_2$ [b,c])	18+5		28	53	96%
	$Ba^{35}Cl_2$ [b])	11+5		15	30	>99%
^{37}Cl(^{13}C, ^{14}O)^{36}P	$Ba^{37}Cl_2$ [b,c])	17+5		31	56	96%
	$Ba^{35}Cl_2$ [b])	11+5		15	30	>99%

[a]) Determined via Rutherford backscattering (150°) of 1.9 MeV protons.

[b]) Target material covered with a thin layer of carbon (~5 μgms/cm^2).

[c]) Material obtained from the conversion of enriched NaCl(^{37}Cl: 98.2%; ^{35}Cl: 99.4%). The ^{35}Cl contamination of the $BaCl_2$ was determined via the 1988 keV resonance in the ^{35}Cl(p, α)^{32}S reaction [12]).

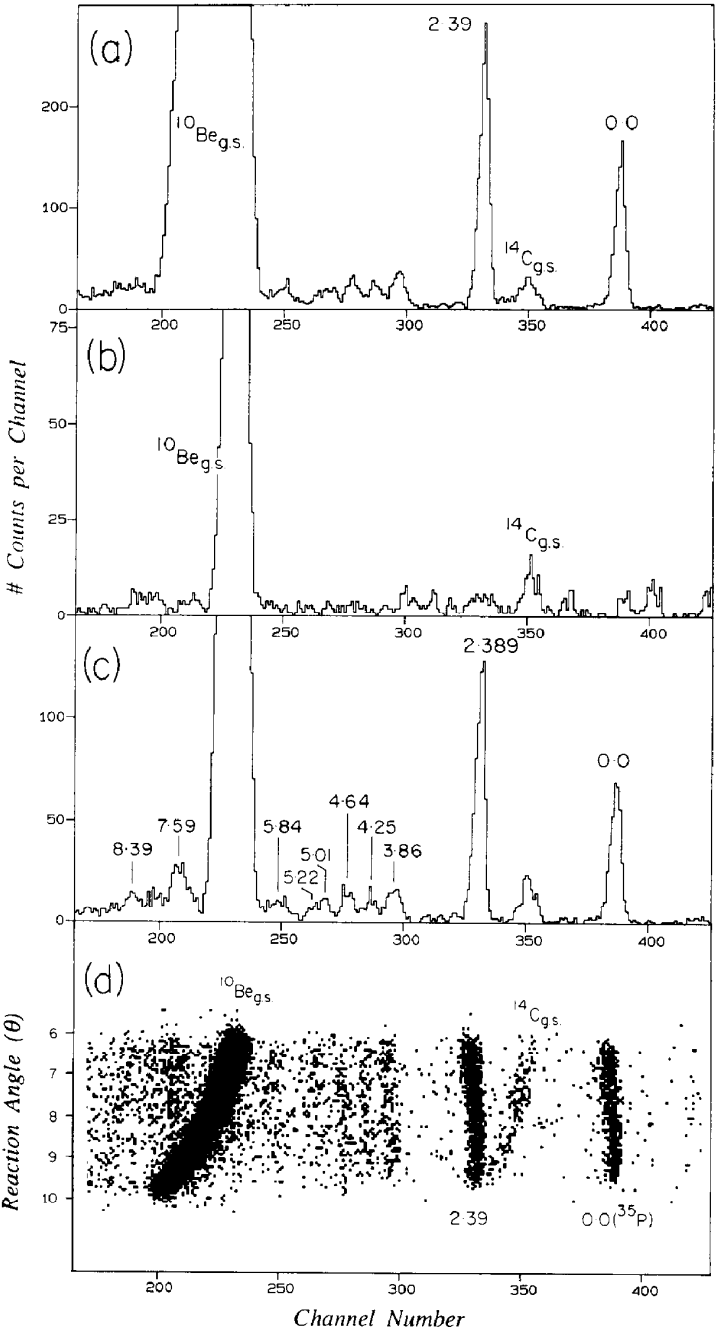

Fig. 1. (a) Position spectrum of $^{13}N^{7+}$ ions from the $^{37}Cl(^{11}B, ^{13}N)^{35}P$ reaction covering the full acceptance aperture of the spectrometer ($\theta = 5.75°$–$10.25°$). (b) Position spectrum from the $^{35}Cl(^{11}B, ^{13}N)^{33}P$ reaction for $^{13}N^{7+}$ ions emitted across the forward half of the spectrometer aperture ($\theta = 5.75°$–$8.0°$). (c) As for (b) but for the $^{37}Cl(^{11}B, ^{13}N)^{35}P$ reaction. (d) Two-dimensional plot of reaction angle (θ) versus position for $^{13}N^{7+}$ ions from (^{11}B, ^{13}N) reactions on the ^{37}Cl target.

found to lose chlorine rapidly when bombarded, while at the same time the oxygen content of the target increased. Similar observations of chlorine losses from metallic chloride targets have been reported by other authors [10,11]). In addition, the deterioration of the targets was greatly accelerated if they had been exposed to air for several days, presumably due to the absorption of water by the hygroscopic $BaCl_2$. The solution to the problem of chlorine loss proved to be the evaporation of a thin ($\sim 5\ \mu g/cm^2$) carbon layer over the barium chloride layer and the storage of the targets in an evacuated desiccator between the time of production and bombardment. Only a single target was required to perform the ^{36}P measurement, during which it was exposed to a total charge of 40 mC of $^{13}C^{6+}$ ions over several days with currents reaching 300 nA. Throughout the experiment, periodic monitoring of the yield of elastically scattered ions demonstrated that no significant loss of chlorine occurred.

3. Results

3.1. THE $^{37}Cl(^{11}B\ ^{13}N)^{35}P$ REACTION

The position spectra of $^{13}N^{7+}$ ions produced in the $^{35,37}Cl(^{11}B, ^{13}N)^{33,35}P$ reactions are shown in fig. 1a–c. These spectra display an energy resolution of 200 keV (fwhm). The reaction cross section, averaged over the entrance aperture of the spectrometer, is 0.12 mb/sr for the population of the ^{35}P ground state and 0.20 mb/sr for the first excited state.

A calibration of the focal plane was carried out using the $^{35}Cl(^{11}B, ^{12}C)^{34}S$ reaction, for which a $^{11}B^{4+}$ beam of the same magnetic rigidity as the 81 MeV $^{11}B^{5+}$ beam was employed ($E(^{11}B^{4+}) = 51.91$ MeV). Two sets of data were acquired: one at the same setting of the spectrometer field as used for the (^{11}B, ^{13}N) measurements and the second at a setting which was 3% higher. These resulted in eight points of known Q-value spanning the region of interest (fig. 2). The state labelled "4.883" is in fact a close doublet consisting of the $4.875(3^+)$ and $4.891(2^+)$ MeV states. Any uncertainty introduced by the preferential population of either state is negligible. The 4.072 MeV state is identified on the basis of the corresponding (d, ^{3}He) reaction data of ref. [13]).

Also evident in fig. 1a are broad peaks arising from the (^{11}B, ^{13}N) reaction on the ^{12}C and ^{16}O in the targets. The broadness of these peaks is due to the ^{13}N ejectiles being focused well forward of the position-sensing wire of the focal plane detector. However, by using the angle-of-entry information from the detector (fig. 1d) it is possible to restrict the range of reaction angles accepted and hence to reduce the widths of these contaminant peaks. A spectrum (fig. 1c) corresponding to only the forward half of the spectrometer angular acceptance reveals two states in ^{35}P which are obscured by the ^{10}Be ground state in fig. 1a.

The excitation energies of states in ^{35}P observed in the present work are summarised in table 2.

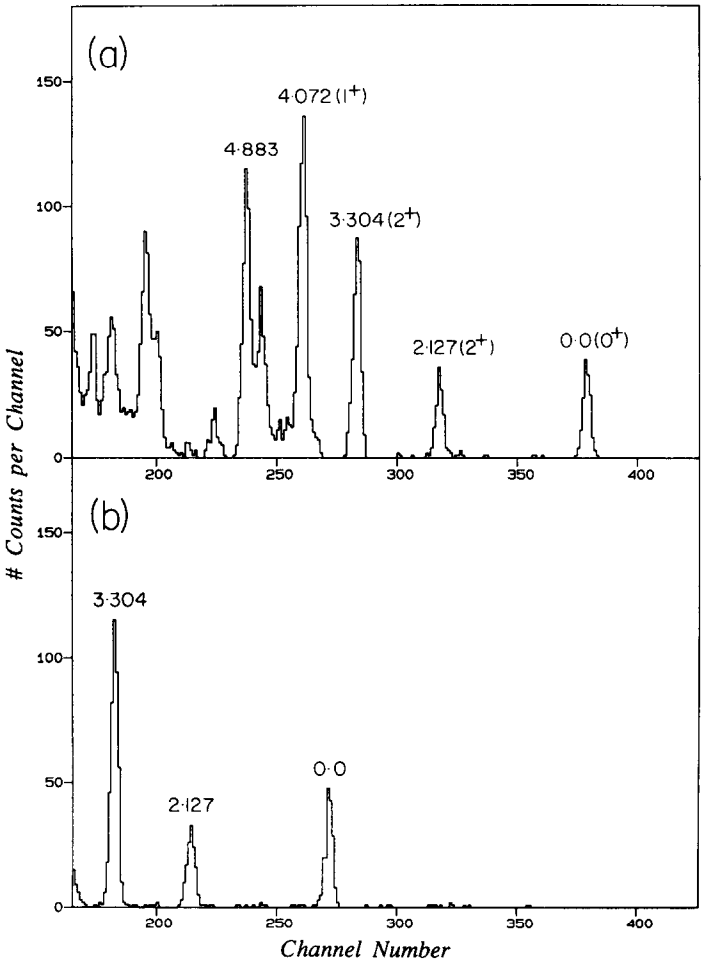

Fig. 2. Position spectra of $^{12}C^{6+}$ ions from the $^{35}Cl(^{11}B, ^{12}C)^{34}S$ reaction at (a) the experimental field setting of the spectrometer, and (b) a field setting 3% higher.

3.2. THE $^{34}S(^{18}O, ^{17}F)^{35}P$ REACTION

Position spectra of $^{17}F^{9+}$ ions from the $^{32,34}S(^{18}O, ^{17}F)^{33,35}P$ reactions are presented in fig. 3. The energy resolution is 250 keV (fwhm) and the average reaction cross section for the population of the ^{35}P ground state is 12 μb/sr.

The calibration of the focal plane in terms of reaction Q-value was achieved using the $^{34}S(^{18}O, ^{20}Ne)^{32}Si$ reaction for which ground state lies 23 mm above that of ^{35}P. As this reaction was slightly out of focus, care was taken to account for any angular distribution effects over the 4.5° acceptance aperture of the spectrometer. This reaction also facilitated the monitoring of any slow drifts in the position spectrum. The dispersion of the focal plane in the region of interest was determined by measuring, at a fixed value of the spectrometer field, elastically scattered ^{18}O ions

TABLE 2

Excitation energies of levels in ^{35}P
E_x [MeV(±keV)]

^{36}S(d, ^{3}He)^{35}P [a])	J^π [a])	^{37}Cl(^{11}B, ^{13}N)^{35}P [b])	^{34}S(^{18}O, ^{17}F)^{35}P [c])
0.0	$\frac{1}{2}^+$	0.0	0.0
2.386 (6)	$\frac{3}{2}^+$	2.389 (4)	2.42 (40)
3.857 (2)	$\frac{5}{2}^+$	3.86 (10)	
		4.25 (20)	
4.474 (21)			
4.665 (3)	$\frac{5}{2}^+$	4.64 (20)	
		5.01 (20)	
			5.07 (40)
5.189 (13)	$\frac{5}{2}^+$	5.22 (40)	
		5.84 (50)	5.89 (70)
			6.44 (60)
			7.05 (60)
			7.44 (60)
7.520 (30)			
		7.59 (20)	
			7.92 (60)
		8.39 (40)	
			8.6 (100)
			9.29 (50)

[a]) Ref. [7]).
[b]) See fig. 1.
[c]) See fig. 3.

for beam energies between 95 and 108 MeV in increments of 1 MeV. Differences in energy loss of the various ion species in the targets were calculated using the tables of Ziegler [14]). The resultant calibration leads to a mass excess of -24.87 ± 0.04 MeV for the ^{35}P ground state and to the excitation energies listed in table 2. This value of the mass excess is in good agreement with the more precise value (-24.859 ± 0.002 MeV) obtained by Khan *et al.* [7]).

The most notable features of the spectrum shown in fig. 3c are the weak population of the ground state and the strong population of levels in the region between 5 and 9.3 MeV. Their significance will be discussed further in sect. 4.1.2.

3.3. THE ^{37}Cl(^{13}C, ^{14}O)^{36}P REACTION

Position spectra of $^{14}O^{8+}$ ions from the ^{35,37}Cl(^{13}C, ^{14}O)^{34,36}P reactions are displayed in fig. 4. The energy resolution is 230 keV (fwhm) – the dominant contribution being the differences in energy loss between the ^{13}C and ^{14}O ions traversing the target.

An absolute calibration of the focal plane spectrum was obtained via the ^{37}Cl(^{13}C, ^{14}N)^{36}S reaction (fig. 5) using a $^{13}C^{5+}$ beam of the same magnetic rigidity as the 94.5 MeV $^{13}C^{6+}$ beam ($E(^{13}C^{5+}) = 65.7$ MeV). Periodic monitoring of elastic scattering from the target of the lower energy beam provided a check, not only on

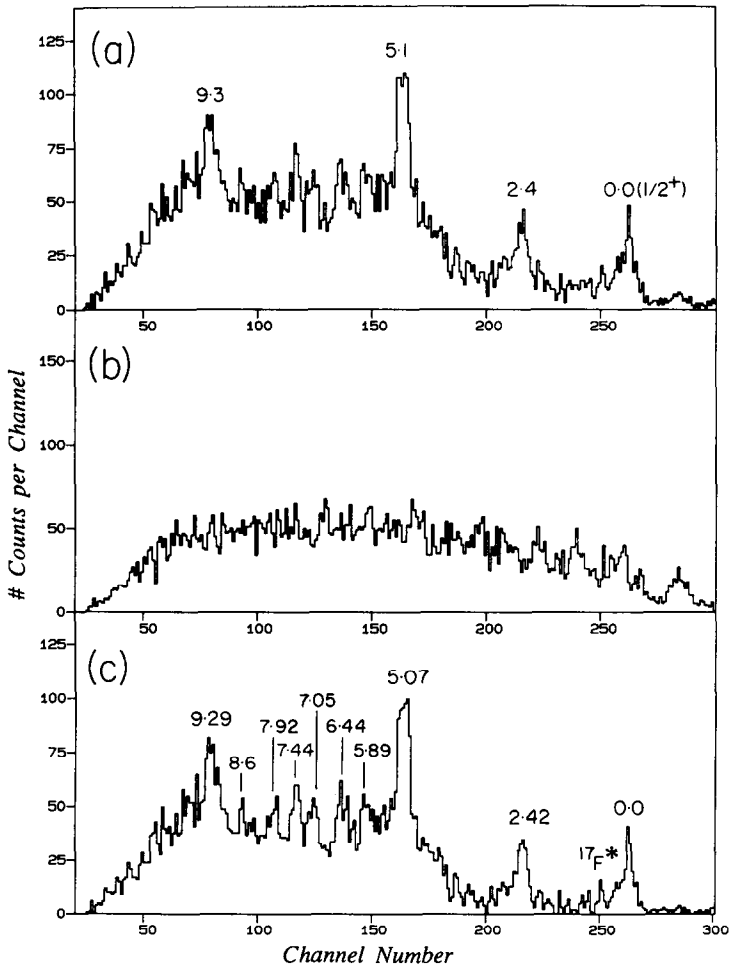

Fig. 3. Position spectra of $^{17}F^{9+}$ ions from (a) the $^{34}S(^{18}O, ^{17}F)^{35}P$ reaction, (b) the $^{32}S(^{18}O, ^{17}F)^{33}P$ reaction, and (c) the $^{34}S(^{18}O, ^{17}F)^{35}P$ reaction after a scaled background subtraction based on the ^{32}S contamination of the $Ag_2{}^{34}S$ target (table 1). The peak labelled $^{17}F^*$ corresponds to the excitation of the ejectile ($E_x = 495$ keV).

the condition of the target, but also on the stability of the position spectrum. The dispersion of the focal plane in the region of interest was acquired through the (^{13}C, ^{14}N) reaction at a slightly higher spectrometer field setting such that the ground state occupied a position previously straddled by the 3.291(2^+) and 4.523(1^+) MeV states of ^{36}S (fig. 5b). Again, corrections were applied to account for differences in energy loss of the various ions in the target. In this manner, a ground state mass excess of -20.21 ± 0.05 MeV was extracted for ^{36}P, in reasonable agreement with the value of -20.25 MeV obtained in the two earlier measurements [2,5]), whilst being $\sim$0.7 MeV less bound than the Garvey-Kelson prediction [15]). The cross section for

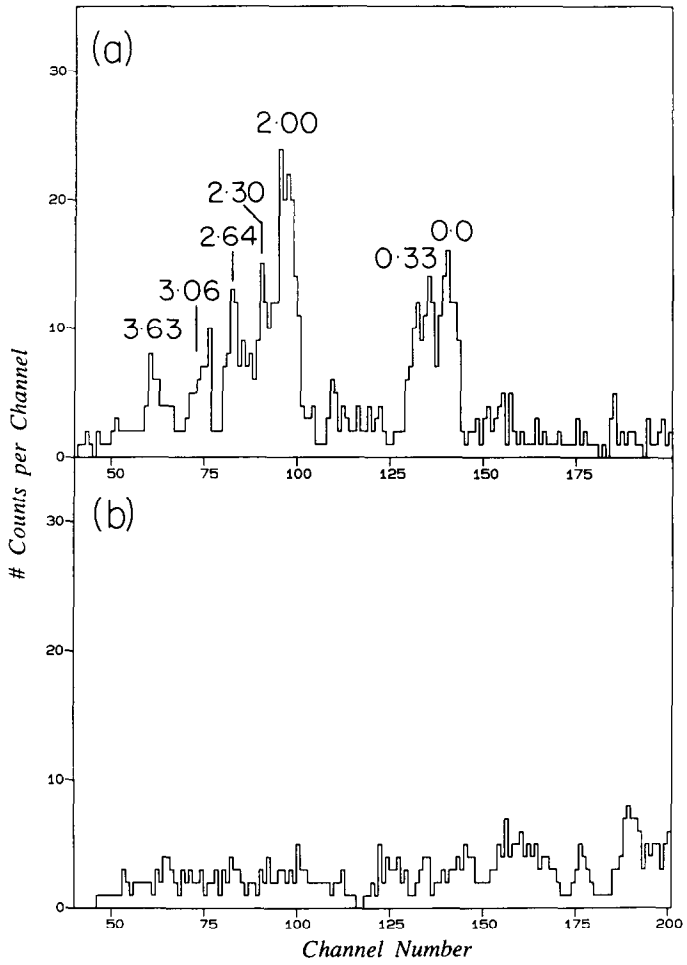

Fig. 4. Position spectra of $^{14}O^{8+}$ ions from (a) the $^{37}Cl(^{13}C, ^{14}O)^{36}P$ and (b) $^{35}Cl(^{13}C, ^{14}O)^{34}P$ reactions.

the population of the ^{36}P ground state through the (^{13}C, ^{14}O) reaction at 8.0° is 1 μb/sr.

In addition to the ground state, a number of peaks are visible in the spectrum up to the cut-off in detector acceptance at ~4 MeV. The excitation energies determined for these states are given in table 3. The broadness of the feature at 0.33 MeV indicates that it may be an unresolved doublet (sect. 4.2).

4. Discussion

4.1. ^{35}P

The structure of ^{35}P has previously been investigated through the (d, ^{3}He) studies of refs. [6,7]), leading to spin and parity assignments for 5 levels up to 5.2 MeV in ^{35}P.

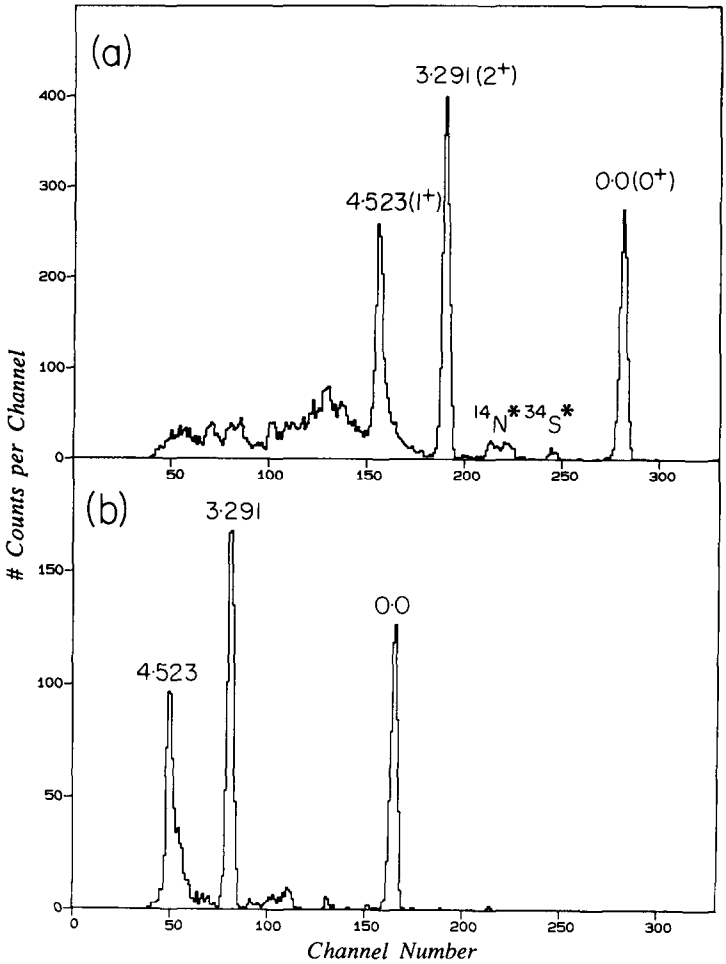

Fig. 5. Position spectra of $^{14}N^{7+}$ ions from the $^{37}Cl(^{13}C, ^{14}N)^{36}S$ reaction at (a) the experimental field setting of the spectrometer, and (b) a field setting 3.5% higher.

These results are summarised in fig. 6, which also shows the energy levels observed in the present work, as well as the predicted level schemes of the $(sd)^{-5}$ shell model calculations of Wildenthal [16]) and of simple weak-coupling calculations [6,17]). The most notable feature of the (d, ^{3}He) studies is the observation of three $\frac{5}{2}^+$ levels with appreciable proton pick-up strength where only one is expected from the shell-model calculations. This has been interpreted [6]) as evidence for mixing between the $(sd)^{-5}$ shell-model state and two $2\hbar\omega$ weak coupling states which are predicted to lie close in excitation energy. The $\frac{3}{2}^+$ state at 2.386 MeV is weakly populated by the (d, ^{3}He) reaction, as expected if the proton configuration of the ^{36}S ground state is predominantly $(d_{5/2})^6(s_{1/2})^2$.

TABLE 3

Excitation energies of levels in ^{36}P
E_x [MeV(±keV)]

$^{36}S(^{7}Li, ^{7}Be)^{36}P$ [a]	$^{36}S(^{14}C, ^{14}N)^{36}P$ [b]	$^{37}Cl(^{13}C, ^{14}O)^{36}P$ [c]
0.0	0.0	0.0
0.252 (10)		
		0.33 (20) [d]
	0.450 (22)	
		2.00 (20)
		2.30 (30)
		2.64 (30)
		3.06 (30)
		3.63 (30)

[a]) Ref. [2]).
[b]) Ref. [5]).
[c]) See fig. 4.
[d]) Doublet (sect. 4.2).

4.1.1. The $^{37}Cl(^{11}B, ^{13}N)^{35}P$ reaction. Owing to the presence of a $1d_{3/2}$ proton in the ground state of ^{37}Cl, the 2-proton pick-up reaction is expected to populate, in addition to the states populated by the single proton pick-up reactions, states in ^{35}P in which one of the protons is in the $1d_{3/2}$ orbit. This expectation is borne out by the strong population of the $\frac{3}{2}^+$ state at 2.39 MeV.

In order to place these statements on a more quantitative footing, DWBA calculations have been performed for the 2-proton pickup reaction using the exact finite-range code SATURN-MARS [18]). Optical-model parameters were taken from a $^{11}B+^{27}Al$ study [19]) at 79.5 MeV for the entrance channel and from $^{14}N+^{28}Si$ at 84 MeV [ref. [20])] for the exit channel. The depth of the bound state potential was adjusted to reproduce the binding energy of the di-proton cluster in the target and ejectile. Table 4 lists the optical model and bound state parameters employed in the calculations. Spectroscopic factors were calculated from the shell model using the code OXBASH [21]). The (6-16) 2BME interaction of Cohen and Kurath [22]) was used for ^{11}B and ^{13}N and the universal s-d shell interaction of Wildenthal [16]) for ^{37}Cl and ^{35}P. Calculated cross sections were integrated over the 4.5° angular acceptance of the spectrometer for comparison with experiment. This comparison is shown in table 5.

The first point to note is that the fragmentation of the $\frac{5}{2}^+$ strength in ^{35}P observed in the single-proton pick-up reactions is also observed in the 2-proton pick-up reaction. Secondly, the absolute magnitude of the calculated cross section for the $\frac{1}{2}^+$ ground state is in reasonable agreement with observation given the experimental uncertainty (estimated to be 25%) and the inherent uncertainties in the optical-model parameters. This agreement extends to the $\frac{5}{2}^+$ states if the sum of the strengths to the three levels is used and suggests that at these energies the (^{11}B, ^{13}N) reaction

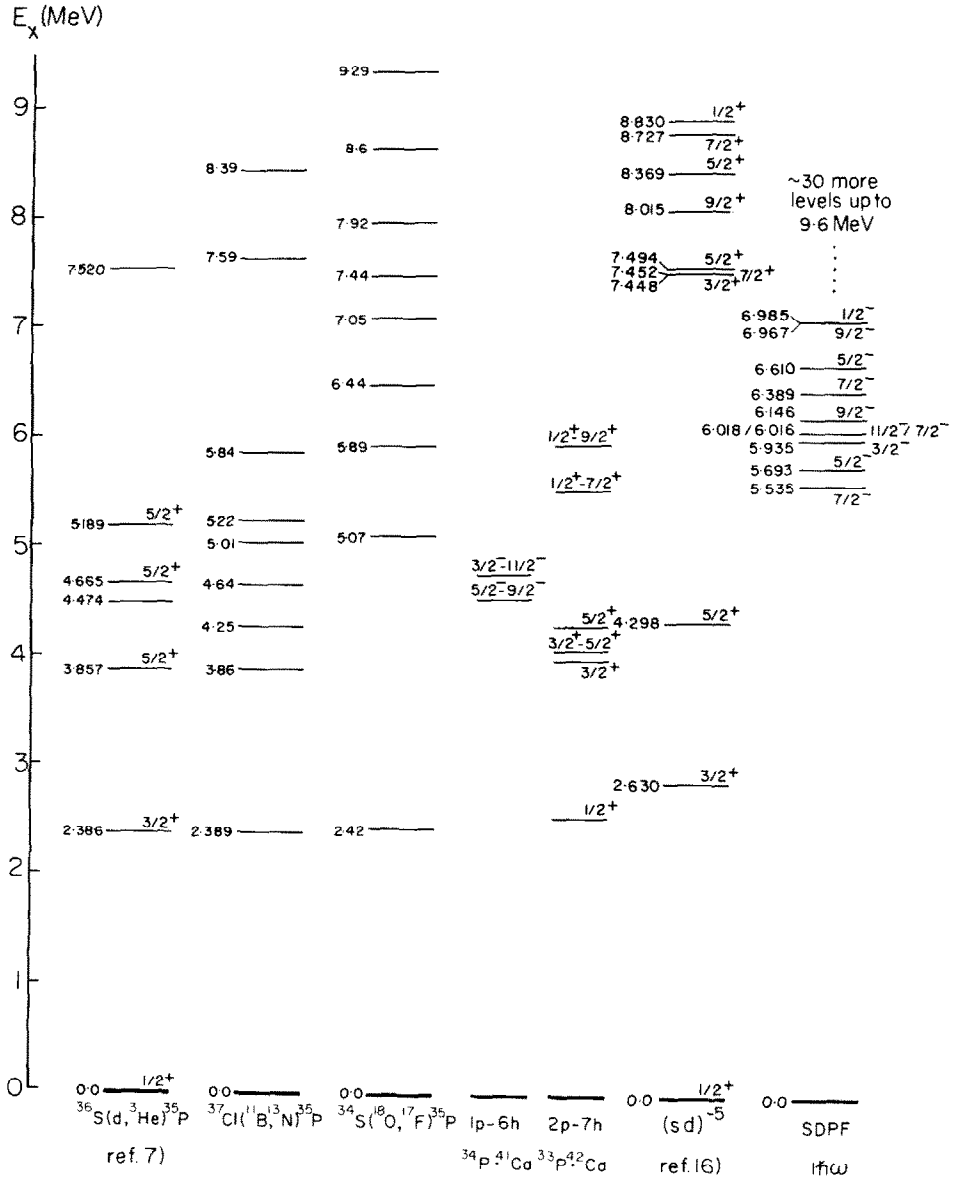

Fig. 6. A comparison of the levels in ^{35}P observed in the present work with those determined from a previous reaction study [7]) and with the results of $0\hbar\omega$ $(sd)^{-5}$ [ref. [16])] and $1\hbar\omega$ shell-model calculations. Also shown are the predictions of the weak-coupling model [6,17]).

TABLE 4

Optical-model parameters used in DWBA calculations for the ^{37}Cl(^{11}B, ^{13}N)^{35}P reaction

	V_r [a] (MeV)	r_r (fm)	a_r (fm)	$V_{s.o.}$ [b] (MeV)	$r_{s.o.}$ (fm)	$a_{s.o.}$ (fm)	V_i [a] (MeV)	r_i (fm)	a_i (fm)	r_C [c] (fm)
entrance channel	10.0	1.300	0.803	0.0	0.0	0.0	30.2	1.230	0.577	1.223
exit channel	60.0	1.148	0.527	0.0	0.0	0.0	14.0	1.164	0.929	0.834
bound state	Searched	1.250	0.650	7.0	1.250	0.650	0.0	0.0	0.0	1.250

[a]) $V_x(r) = V_x[\exp\{(r - r_x A_t^{1/3})/a_x\} + 1]^{-1}$, x = r or i and t = target.
[b]) $V_{s.o.}(r)$ = real Woods-Saxon derivative spin-orbit potential.
[c]) $V_C(r)$ = Coulomb potential of a spherical, uniform distribution of radius $r_C A_t^{1/3}$.

TABLE 5

Comparison of the ^{37}Cl(^{11}B, ^{13}N)^{35}P reaction data with shell-model and DWBA calculations

Experimental results			Predictions		
E_x [MeV]	J^π [a]	$\langle d\sigma/d\omega \rangle$ [μb/sr] $\pm \sim 25\%$	E_x [MeV] [b]	J^π [b]	$\langle d\sigma/d\omega \rangle$ [μb/sr]
0.0	$\frac{1}{2}^+$	120	0.0	$\frac{1}{2}^+$	80
2.389	$\frac{3}{2}^+$	200	2.630	$\frac{3}{2}^+$	90
3.86	$\frac{5}{2}^+$	35			
4.64	$\frac{5}{2}^+$	30 } 75	4.298	$\frac{5}{2}^+$	65
5.22	$\frac{5}{2}^+$	$\sim$10			
7.59		45	7.452	$\frac{7}{2}^+$	40

[a]) Ref. [7]).
[b]) Ref. [16]).

proceeds predominantly via the transfer of a di-proton cluster. The calculations for the $\frac{3}{2}^+$ state at 2.39 MeV correctly predict that this state should be the most strongly populated, but under-estimate the absolute cross section by a factor of two.

Additional states at 4.25 and 5.01 MeV, which are not observed in the single-proton pick-up reactions, are populated by the (^{11}B, ^{13}N) reaction. These may be $\frac{3}{2}^+$ states of predominantly 2p-7h character which are populated via small components of the single-particle shell-model state in their wavefunctions. If so, the much weaker mixing of the $\frac{3}{2}^+$ states compared with the $\frac{5}{2}^+$ states can probably be attributed to a greater separation between the $\frac{3}{2}^+$ $(sd)^{-5}$ shell model state and the 2p-7h $\frac{3}{2}^+$ states.

At higher excitation energy, there is a state at 7.59 MeV which is moderately strongly excited. Comparison with the shell model and DWBA calculations (table 5) indicates that this level is a candidate for the first $\frac{7}{2}^+$ state.

4.1.2. The ^{34}S(^{18}O, ^{17}F)^{35}P reaction. The spectrum from this reaction (fig. 3) displays a number of interesting features. Of particular note is the population with approximately equal strength of the ground ($\frac{1}{2}^+$) and 2.39 MeV ($\frac{3}{2}^+$) states, in contrast to the single proton pick-up reactions [2,5–7]) in which the former is much more strongly

populated. This relative enhancement of the $\frac{3}{2}^+$ state is probably due in part to the $1d_{3/2}$ proton occupancy being substantially greater in ^{34}S than in ^{36}S [ref. [7])]. It is also of interest to note the suppression of the first two $\frac{5}{2}^+$ states, as indicated by the lack of reaction strength in the vicinity of ~4 MeV.

Most of the strength observed in the ^{34}S(^{18}O, ^{17}F)^{35}P reaction, however, proceeds to states above 5 MeV. As is evident from the $(sd)^{-5}$ shell-model level scheme shown in fig. 6, most of this strength cannot be associated with sd-shell states and the states observed must involve excitations into the fp-shell. Consequently, further shell-model calculations have been performed within a 2s, 1d, 1f, 2p basis to search for $1\hbar\omega$ states in ^{35}P using a new interaction, labelled SDPF, which has recently been described by Warburton *et al.* [23]). This interaction was found to give a good account of the low-lying negative-parity levels in other nuclei near the $N = 20$ shell closure, such as ^{37}Cl and ^{38}Ar. In order to limit the matrix dimensions, the present calculations were performed with the restrictions that there be a minimum of 9 particles in the $1d_{5/2}$ subshell and that the $2p_{1/2}$ and $1f_{5/2}$ subshells be empty. The resulting level scheme is presented in fig. 6 and shows a high density of levels starting at an excitation energy of 5.5 MeV in ^{35}P. However, a study of the wavefunctions of these negative-parity levels reveals that, up to an excitation energy of 9 MeV, they are all predominantly $(d_{5/2})^{12}(s_{1/2})^2(d_{3/2})^4(fp)$. Such configurations are not accessible by single-proton pick-up, 2-neutron stripping on the dominant $(d_{5/2})^{12}(s_{1/2})^4(d_{3/2})^2$ component of the ^{34}S ground state. Hence it is more likely that the strongly excited states observed in the (^{18}O, ^{17}F) reaction are positive-parity $2\hbar\omega$ states rather than negative-parity $1\hbar\omega$ states. Further support for this interpretation is provided by data from two-neutron stripping reactions on ^{34}S targets. These serve to indicate which configurations the two neutrons transferred during the (^{18}O, ^{17}F) reaction are likely to populate. The ^{34}S(t, p)^{36}S reaction has been studied at 3.1 MeV by Olness *et al.* [24]) and the ^{34}S(^{18}O, ^{16}O)^{36}S reaction at 104 MeV in this laboratory (fig. 7). In both reactions the most strongly excited state is the 2^+ level at 4.58 MeV, which is believed to be a predominantly 2p-6h ($2\hbar\omega$) state. There is also appreciable population of several other levels above 5 MeV, few of which can be identified with $0\hbar\omega$ shell-model states. In contrast, the $1\hbar\omega$ 3^- state at 4.19 MeV is only weakly populated.

Thus, in terms of a weak-coupling description, the levels in ^{35}P most strongly excited by the (^{18}O, ^{17}F) reaction may resemble a proton-hole coupled to the neutron configuration analogous to the 4.58 MeV 2^+ level in ^{36}S. Similarly, little strength would be expected to the low-lying negative-parity states. Hence, the prominent feature at 5.07 MeV in ^{35}P may be due to one or both of the states ($\frac{3}{2}^+$ and $\frac{5}{2}^+$) arising from the coupling of a $2s_{1/2}$ proton-hole to the $2\hbar\omega$ (2^+) neutron configuration. The broadness of this peak is such that it would encompass the known $\frac{5}{2}^+$ state at 5.19 MeV, which is principally 2p-7h in character (sect. 4.1), and another state (presumably the $\frac{3}{2}^+$) at lower excitation energy. Extending this picture further, states located above the 5.07 MeV level may be predominantly a $2s_{1/2}$ or $1d_{5/2}$ proton-hole coupled to neutron configurations analogous to the strongly excited states above

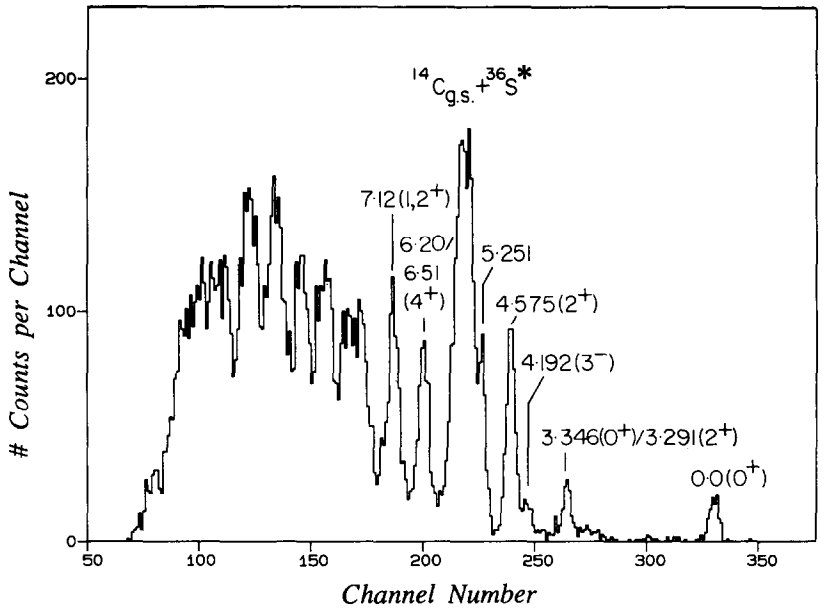

Fig. 7. Position spectra of $^{16}O^{8+}$ ions from the $^{34}S(^{18}O, ^{16}O)^{36}S$ reaction at $E(^{18}O^{7+}) = 104$ MeV and $\langle\theta\rangle = 8.0°$. The peak labelled $^{14}C_{g.s.}+^{36}S^*$ indicates the obscuration of a number of excited states in ^{36}S by the $^{14}C_{g.s.}$.

5 MeV in ^{36}S. As shown in fig. 6, the location of 1p-6h and 2p-7h multiplets has been estimated using the weak-coupling model [6,17]).

4.1.3. Comparison with γ-ray data. Dufour *et al.* [8]) have recently studied the γ-rays emitted following the β-decay of a number of neutron-rich nuclei including ^{35}Si. They have tabulated the energies and intensities of the γ-rays observed but have not placed them in a decay scheme.

The ^{35}Si ground state is expected to have spin and parity $\frac{7}{2}^-$, whence the states in ^{35}P fed by allowed β-decay will be negative-parity $\frac{5}{2}^-$ to $\frac{9}{2}^-$ states. From the $1\hbar\omega$ shell-model calculations presented above, these levels are expected to have excitation energies in excess of 5.5 MeV but, because of the multipolarities involved would not be expected to γ-decay to the $\frac{1}{2}^+$ ground state. Certainly no transitions with energies greater than 4.1 MeV were observed by Dufour *et al.* [8]). A tentative decay scheme based on their data and the information from single-proton pick-up reactions is shown in fig. 8. Only the 2386 and 3860 keV levels can be definitely associated with levels observed in nuclear reactions, although a weakly-populated level at 4474 ± 21 keV observed by Khan *et al.* [7]) may be the same as the proposed 4493 keV level in fig. 8. In addition a weak level at 4105 ± 19 keV has been observed by the McMaster group in the $^{36}S(t, \alpha)^{35}P$ reaction [25]). The existence of levels at 6488 and 7450 keV is supported by the observation of states at 6.44 and 7.44 MeV in the (^{18}O, ^{17}F) reaction.

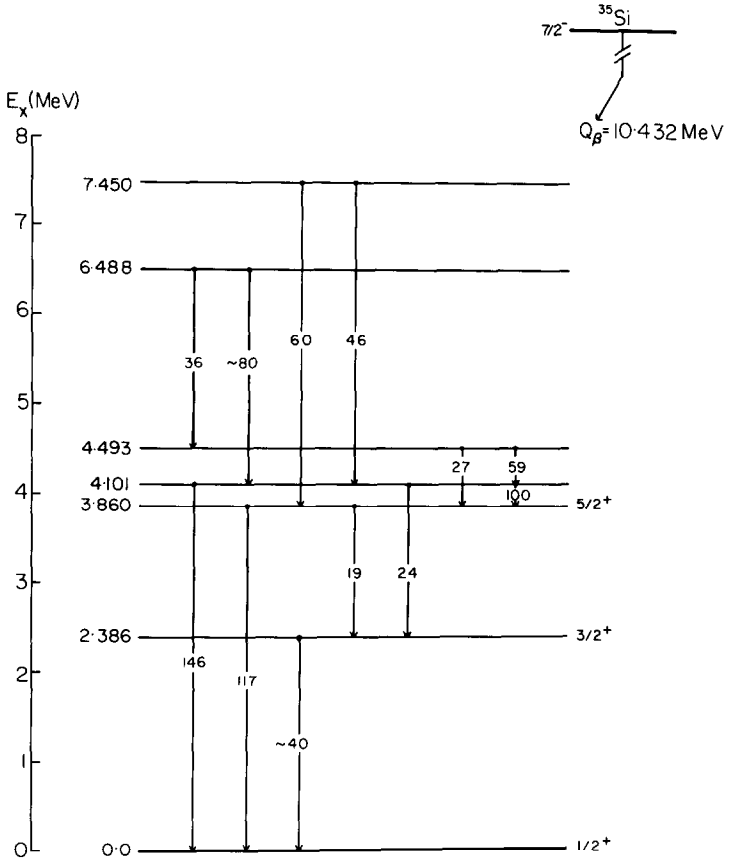

Fig. 8. Proposed decay scheme for ^{35}P based upon γ-ray energies and intensities observed following the β-decay of ^{35}Si [ref. [8])].

In the proposed decay scheme, there is more γ-ray strength leaving than entering all of the excited states except the 3860 keV level. However, for the states below 4.5 MeV this imbalance should not necessarily be interpreted as evidence for direct β-feeding to these levels, which probably have positive parity. Rather, it is more likely that the anticipated high density of negative-parity levels above 6 MeV results in a number of weaker transitions feeding into these lower-lying levels, which were not observed by Dufour *et al.* [8]). The 3174 keV transition cannot be fitted unambiguously into the decay scheme but, on the basis of intensity balances it could be due to a transition to either the 4101 or 4493 keV levels. Confirmation of this tentative decay scheme will require further measurements, in particular of $\gamma\gamma$-coincidences.

4.2. ^{36}P

Previous information on ^{36}P has been obtained from two studies [2,5]) of charge exchange reactions on ^{36}S targets. The ground state masses measured in both studies

are in good agreement, but different excited states were observed in the two cases. One study [2]), employing both the (^{7}Li, ^{7}Be) and (^{11}B, ^{11}C) reactions, observed only the one excited state at 252 ± 10 keV. The other [5]), employing the (^{14}C, ^{14}N) reaction, observed only a single level at 450 ± 22 keV. These two levels were not resolved in the present study, however the observation of a broadened peak centred at 0.33 MeV indicates that both levels are populated with approximately equal strength via the

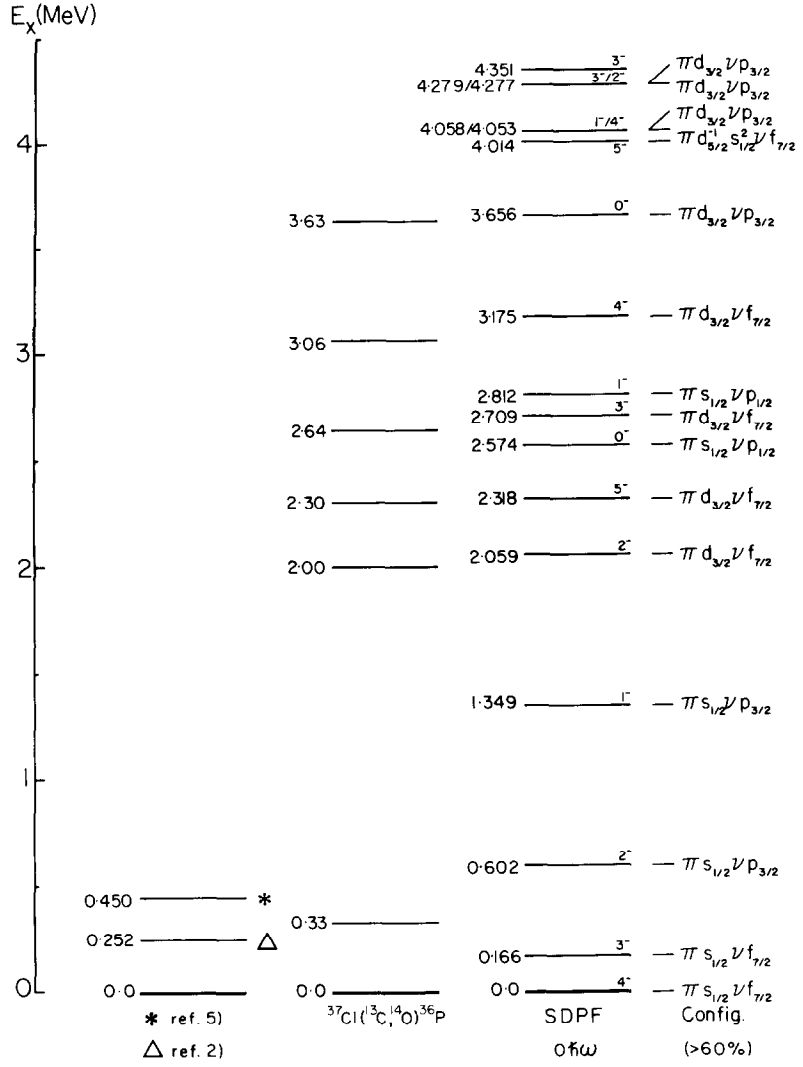

Fig. 9. A comparison of the levels in ^{36}P observed in the present study with those determined from charge-exchange reaction studies [2,5]) and with the results of a 0ħω shell-model calculation. Also shown are the dominant (>60%) configuration of each of the shell-model states.

^{37}Cl(^{13}C, ^{14}O)^{36}P reaction. In addition, a number of other levels which were not observed in the charge exchange reactions are populated.

Fig. 9 shows the experimental level scheme of ^{36}P as determined from the (^{13}C, ^{14}O) reaction and compares it with a shell-model calculation employing the SDPF interaction in a complete 2s, 1d, 1f, 2p basis (sect. 4.1.2). Also shown are the dominant components (greater than 60%) of the shell-model wavefunctions relative to a core with a closed neutron shell and a full $1d_{5/2}$ proton subshell. The weak coupling structure of the shell-model wavefunctions is obvious. Furthermore the centroids of the $\pi s_{1/2}\nu f_{7/2}$ and $\pi d_{3/2}\nu f_{7/2}$ multiplets are separated by 2.48 MeV, which is to be compared with the 2.39 MeV separation between the $2s_{1/2}$ and $1d_{3/2}$ single-particle states in ^{35}P. Similarly, the 0.89 MeV separation between the $\pi s_{1/2}\nu f_{7/2}$ and $\pi s_{1/2}\nu p_{3/2}$ doublets compares favourably with the 0.64 MeV separation of the $\frac{7}{2}^-$ and $\frac{3}{2}^-$ states in ^{37}S.

The charge exchange reactions are not expected to populate those states which have a predominantly $d^6_{5/2}d_{3/2}$ proton configuration owing to the small probability of finding the $d^6_{5/2}d^2_{3/2}$ proton configuration in the ^{36}S ground state. This is certainly in line with observation if the three levels observed are associated with the lowest three shell-model levels as shown in fig. 9. It is far from obvious why the (^{7}Li, ^{7}Be) and (^{11}B, ^{11}C) reactions should populate the two lower levels with equal intensity, whereas the 252 keV level is not seen at all in the (^{14}C, ^{14}N) reaction.

In contrast to the charge exchange reactions, the (^{13}C, ^{14}O) reaction can populate states in ^{36}P having a proton in the $1d_{3/2}$ orbit because the two protons picked up in this reaction may both be taken from the $2s_{1/2}$ orbit leaving a $1d_{3/2}$ proton behind. Consequently, the (^{13}C, ^{14}O) reaction should populate not only the levels seen in the charge exchange reactions, but also the members of the $\pi d_{3/2}\nu f_{7/2}$ multiplet. Remarkably, a comparison of the experimental and shell model level schemes in fig. 9 shows that there is an experimental candidate at very nearly the predicted energy for almost all the members of the $\pi s_{1/2}\nu f_{7/2}$, $\pi s_{1/2}\nu p_{3/2}$ and $\pi d_{3/2}\nu f_{7/2}$ multiplets - the single exception being the 1^- $\pi s_{1/2}\nu p_{3/2}$ level.

Dufour *et al.* [8]) have observed γ-rays emitted following the β-decay of ^{36}Si with energies of 250 and 425 keV, in accord with the existence of low-lying levels at these energies. The additional observation of a 175 keV γ-ray line can be attributed to a transition between the two levels.

5. Conclusions

The multi-nucleon transfer reactions ^{37}Cl(^{11}B, ^{13}N)^{35}P, ^{34}S(^{18}O, ^{17}F)^{35}P and ^{37}Cl(^{13}C, ^{14}O)^{36}P have been used to study the spectroscopy of the nuclei ^{35}P and ^{36}P. The comparison of the results with DWBA and shell-model calculations has allowed the probable nature of a number of the excited states to be determined. The availability of γ-ray energies following the β-decay of ^{35}Si has allowed a

tentative level scheme to be constructed for ^{35}P. Previous, apparently contradictory results, concerning the lowest levels in ^{36}P have been reconciled.

We wish to thank A. Muggleton for producing the targets used in these experiments; J. Broomhead (Dept. Chemistry, ANU) for assistance in the conversion of the enriched $Na^{37}Cl$ to $Ba^{37}Cl_2$; D. Pringle and W. Vermeer (Nuclear Physics Laboratory, Oxford) for their involvement in the early phase of these measurements; and G. Gilmour for assistance in the production of the figures.

References

1) L.K. Fifield, C.L. Woods, R.A. Bark, P.V. Drumm and M.A.C. Hotchkis, Nucl. Phys. **A440** (1985) 531
2) P.V. Drumm, L.K. Fifield, R.A. Bark, M.A.C. Hotchkis, C.L. Woods and P. Maier-Komor, Nucl. Phys. **A441** (1985) 95
3) L.K. Fifield, C.L. Woods, W.N. Catford, R.A. Bark, P.V. Drumm and K.T. Keoghan, Nucl. Phys. **A453** (1986) 497
4) D.R. Goosman and D.E. Alburger, Phys. Rev. **C6** (1972) 820
5) W.A. Mayer, W. Henning, R. Holzwarth, H.J. Körner, G. Korschinek, W.U. Mayer, G. Rosner and H.J. Scheerer, Z. Phys. **A319** (1984) 287
6) C.E. Thorn, J.W. Olness, E.K. Warburton and S. Raman, Phys. Rev. **C30** (1984) 1442
7) S. Khan, Th. Kihm, K.T. Knöpfle, G. Mairle, V. Bechtold and L. Friedrich, Phys. Lett. **156B** (1985) 155
8) J.P. Dufour, R. Del Moral, A. Fleury, F. Hubert, D. Jean, M.S. Pravikoff, H. Delagrange, H. Geissel and K.-H. Schmidt, Z. Phys. **A324** (1986) 487
9) T.R. Ophel and A. Johnston, Nucl. Instr. Meth. **157** (1978) 461
10) B.M. Paine, S.R. Kennett and D.G. Sargood, Phys. Rev. **C17** (1978) 1550
11) F.C. Erne and P.M. Endt, Nucl. Phys. **71** (1965) 593
12) B. Bosnjakovic, J. Bouwmeester, J.A. Van Best and H.S. Pruys, Nucl. Phys. **A110** (1968) 17
13) N.G. Puttaswamy and J.L. Yntema, Phys. Rev. **177** (1969) 1624
14) J.F. Ziegler, Handbook of stopping cross sections for energetic ions in all elements, vol. 5 (Pergamon, New York, 1980)
15) N.A. Jelley, J. Cerny, D.P. Stahel and K.H. Wilcox, Phys. Rev. **C11** (1975) 2049
16) B.H. Wildenthal, private communication, June 1983; Prog. Part. Nucl. Phys. **11** (1984) 5
17) R.K. Bansal and J.B. French, Phys. Lett. **11** (1964) 145
18) T. Tamura and K.S. Low, Comp. Phys. Comm. **8** (1974) 349
19) C.B. Fulmer, S. Mukhopadhyay, G.R. Satchler, R.L. Auble, J.B. Ball, F.E. Bertrand, E.E. Gross and D.C. Hensley, Nucl. Phys. **A385** (1982) 83
20) C.M. Perey and F.G. Perey, Atomic Data Nucl. Data Tables **17** (1976) 1
21) W.D.M. Rae, A. Etchegoyen, N.S. Godwin and B.A. Brown, OXBASH, The Oxford-Buenos Aires shell model code, internal report, Nov. 1983, Cyclotron Laboratory, Michigan State University
22) S. Cohen and D. Kurath, Nucl. Phys. **A101** (1967) 1
23) E.K. Warburton, D.E. Alburger, J.A. Becker, B.A. Brown and S. Raman, Phys. Rev. **C34** (1986) 1031
24) J.W. Olness, W.R. Harris, A. Gallmann, F. Jundt, D.E. Alburger and D.H. Wilkinson, Phys. Rev. **C3** (1971) 2323
25) N.J. Davis, J.A. Kuehner, A.J. Trudel, C. Bamber, M.C. Vetterli and A.A. Pilt, McMaster Accelerator Laboratory Annual Report (1985) p. 22